Controlling chaos using time delay coordinates via stabilization of periodic orbits

Paul So* and Edward Ott†
University of Maryland, College Park, Maryland 20742
(Received 15 August 1994)

Using time delay coordinates and assuming no *a priori* knowledge of the dynamical system, we propose a method that stabilizes a desired periodic orbit embedded in a chaotic attractor. Similar to the original control algorithm introduced by Ott, Grebogi, and Yorke [Phys. Rev. Lett. **64**, 1196 (1990)], the stabilization is done via small time dependent perturbations of an accessible control parameter. The control method is numerically illustrated using both the Ikeda map, which describes the dynamics of a nonlinear laser cavity and the double rotor map which describes a periodically kicked dissipative mechanical system.

PACS number(s): 05.45.+b

I. INTRODUCTION

In experimental studies of chaotic dynamical systems, it is often the case that the only accessible information is a time series of some scalar function $\xi(\mathbf{X}(t)) = \xi(t)$ of a d-dimensional state variable $\mathbf{X}(t)$. Using delay coordinate embedding technique, Takens [2] showed that a delay coordinate vector

$$\mathbf{Z}(t) = (\xi(t), \xi(t - T_D), \xi(t - 2T_D), ..., \xi(t - MT_D)), \tag{1}$$

with a conveniently chosen delay time T_D and a sufficiently large M, is generically a global one-to-one representation of the system state $\mathbf{X}(t)$. Using a Poincarè surface of section, we obtain a set of discrete state variables $\mathbf{Z}_n = \mathbf{Z}(t_n)$, where $t = t_n$ denotes the time at the nth orbit crossing of the surface of section. As pointed out by Dressler and Nitsche [3], in the presence of parametric variation, delay coordinate embedding leads to a map that in general will depend on all parametric changes that were in effect in the time interval $t_n \leq t \leq t_n - MT_D$. The question that we address is the following: Given a chaotic system reconstructed from time delay coordinates, how can we incorporate dependences of past parametric variations in a control scheme so that a desired attracting time-periodic motion can be attained? This problem was previously addressed by Dressler and Nitsche [3] for the case of a period-one orbit of the Poincarè map in which there was a one-dimensional stable manifold and a one-dimensional unstable manifold.

Similar to the control method originally purposed by Ott *et al.* [1], we wish to make only small controlling perturbations to the system. We do not envision creating new orbits with very different properties from the already existing orbits. Thus we seek to exploit the already existing unstable periodic orbits that are embedded in the chaotic attractor. Controlled chaotic systems offer an advantage in flexibility that any one of a number of different orbits can be stabilized by the small control, and the choice can be switched from one periodic orbit to another without drastically altering the system configuration. The present paper extends previous work [4] to the case when the future system state of a chaotic system depends on the current parametric variation as well as the previous parametric variations.

To numerically illustrate our method, we apply it to both a two-dimensional example, the Ikeda map, and a four-dimensional example, the double rotor map. Physically, the Ikeda map describes the dynamics of a nonlinear optical cavity and the double rotor map describes a periodically forced mechanical system, the kicked double rotor. In the case of the Ikeda map, the stabilization is achieved by small variations of the amplitude of the light pulses entering the optical cavity. To control the double rotor map, stabilization is achieved by small variations of the strength of the periodic forcing.

II. DESCRIPTION OF THE METHOD

To be specific, we concentrate our discussion on a periodically forced system and use a stroboscopic surface of section $t_n = nT_F + t_0$, where T_F is the forcing period. Assume that the orbit of this periodically forced system pierces the experimental surface of section r times in the time interval $t_n < t \leq t_n - MT_D$, when the delay coordinate vector $\mathbf{Z}_n$ is being formed. Then, at the next piercing of the surface of section, the discrete state variable $\mathbf{Z}_{n+1}$ must depend not only on the current value of the forcing p_n, but also on the r previous forcings $p_{n-1}, ..., p_{n-r}$. [We assume that the time-dependent parameter $p(t)$ is constant in each forcing period $p(t) = p_n$ for $t_n \geq t > t_{n-1}$.] Thus the relevant surface of section map will in general be of the form

*Permanent address: Department of Physics and Institute for Plasma Research, University of Maryland, College Park, MD 20742.
†Department of Electrical Engineering and Institute for Systems Research, University of Maryland, College Park, MD 20742.

$$\mathbf{Z}_{n+1} = \mathbf{G}(\mathbf{Z}_n, p_n, p_{n-1}, ..., p_{n-r}). \quad (2)$$

The most direct way to control a nontrivial period T orbit of the map is to take the Tth iterate of the map and apply the method developed in Sec. 2.6 of Ref. [4]. However, this method will be overly sensitive to noise, especially when long-period periodic orbits are involved. The following is a method that we think in general will be better. Control is applied at each iterate of the map instead of each period T. This reduces the chance of the orbit being kicked out of the control region by noise while we are waiting for the orbit to cycle through the T periodic points.

Given a period T periodic orbit $\mathbf{Z}_n^*$ with $\mathbf{Z}_{n+T}^* = \mathbf{Z}_n^*$ and with $p(t) \equiv \bar{p}$ for all t, we can define the following set of $(d \times d)$-dimensional matrices $\mathbf{A}_n$ and a collection of d-dimensional column vectors $\mathbf{B}_n^1, ..., \mathbf{B}_n^{r+1}$ to describe the effect of small control parameter perturbations on the linear dynamics of the surface of section map Eq. (2) near the periodic orbit:

$$\mathbf{A}_n = \mathbf{A}_{n+T} = \mathbf{D}_{\mathbf{Z}}\mathbf{G}(\mathbf{Z}, p_n, p_{n-1}, ..., p_{n-r}), \quad (3a)$$
$$\mathbf{B}_n^1 = \mathbf{B}_{n+T}^1 = \mathbf{D}_{p_n}\mathbf{G}(\mathbf{Z}, p_n, p_{n-1}, ..., p_{n-r}), \quad (3b)$$
$$\mathbf{B}_n^2 = \mathbf{B}_{n+T}^2 = \mathbf{D}_{p_{n-1}}\mathbf{G}(\mathbf{Z}, p_n, p_{n-1}, ..., p_{n-r}), \quad (3c)$$
$$\vdots$$
$$\mathbf{B}_n^{r+1} = \mathbf{B}_{n+T}^{r+1} = \mathbf{D}_{p_{n-r}}\mathbf{G}(\mathbf{Z}, p_n, p_{n-1}, ..., p_{n-r}). \quad (3d)$$

The partial derivatives defined above are all evaluated at $\mathbf{Z} = \mathbf{Z}_n^*(\bar{p})$ and $p_n = p_{n-1} = \cdots = p_{n-r} = \bar{p}$, which is the unperturbed parameter value of the system. For values of p close to $\bar{p}$ and for $\mathbf{Z}_n$ close to the periodic orbit $\mathbf{Z}_n^*(\bar{p})$, the surface of section map Eq. (2) can then be approximated by its linearization

$$\begin{aligned}\mathbf{Z}_{n+1} - \mathbf{Z}_{n+1}^*(\bar{p}) = \mathbf{A}_n[\mathbf{Z}_n - \mathbf{Z}_n^*(\bar{p})] \\ + \mathbf{B}_n^1(p_n - \bar{p}) + \mathbf{B}_n^2(p_{n-1} - \bar{p}) \\ + \cdots + \mathbf{B}_n^{r+1}(p_{n-r} - \bar{p}). \quad (4)\end{aligned}$$

We emphasize that the location of the periodic orbit and the partial derivatives Eq. (3) can be obtained directly from experimental time series. In particular, the location of the periodic orbit and the associated Jacobians $\mathbf{A}_n$ can be extracted from experimental time series using the standard method described in Refs. [5–10]. The collection of matrices $\mathbf{B}_n^j, 1 \le j \le r+1$, that describes the variations of the map Eq. (2) with respect to the different past parametric perturbations can also be obtained experimentally from time series generated by intermittently turning on the parametric perturbations $\delta p = p - \bar{p}$ at each $(r+1)$th piercing of the surface of section (i.e., $\delta p_n = \delta p_{max} \neq 0$ for every n divisible by $r+1$ and $\delta p_n = 0$ otherwise). (We assume δp_{max} to be small enough that the linear approximation is valid.) The next step in finding the matrices $\mathbf{B}_n^j$ is to extract sequences of data points $\{\mathbf{Z}_n\}$ that are in the neighborhood of the periodic orbit $\mathbf{Z}_n^*$ (see Ref. [5]). Since we are keeping track of the history of the parametric perturbations, we can classify these sequences of data points into $r+1$ groups according to the time of the parametric perturbations with respect to n. As an example, let us consider all pairs of points $(\mathbf{Z}_n, \mathbf{Z}_{n+1})$ with $\delta p_n \neq 0$. (The other r groups of data pairs correspond to cases with $\delta p_{n-1} \neq 0, ...,$ or $\delta p_{n-r} \neq 0$.) Since we have chosen $\delta p_{n-1} = \cdots = \delta p_{n-r} = 0$ for this data set, Eq. (4) reduces to the form

$$\mathbf{Z}_{n+1} - \mathbf{Z}_{n+1}^*(\bar{p}) = \mathbf{A}_n[\mathbf{Z}_n - \mathbf{Z}_n^*(\bar{p})] + \mathbf{B}_n^1 \delta p_n.$$

Then, the d-dimensional column vector $\mathbf{B}_n^1(\mathbf{Z}_n^*, \bar{p})$ can be estimated by least-square fitting the data pairs $(\mathbf{Z}_n, \mathbf{Z}_{n+1})$ to the above equation. The other $\mathbf{B}_n^j$, $2 \le j \le r+1$, can be obtained in a similar fashion using the other r groups of data pairs.

In order to include the dynamical dependence of past parametric variations in Eq. (2) in the consideration of the control law, we first incorporate both the delay coordinate vector $\mathbf{Z}_n$ and the r past parametric values into a new $(d+r)$-dimensional state vector $\mathbf{Y}_n$,

$$\mathbf{Y}_n = \begin{pmatrix} \mathbf{Z}_n \\ p_{n-1} \\ p_{n-2} \\ \vdots \\ p_{n-r} \end{pmatrix}. \quad (5)$$

With this new $(d+r)$-dimensional state vector $\mathbf{Y}_n$, we can utilize Eq. (4) to obtain the following matrix equation for the linearized dynamics of the combined "state-plus-parameters" system:

$$\mathbf{Y}_{n+1} - \mathbf{Y}_{n+1}^*(\bar{p}) = \tilde{\mathbf{A}}_n[\mathbf{Y}_n - \mathbf{Y}_n^*(\bar{p})] + \tilde{\mathbf{B}}_n(p_n - \bar{p}), \quad (6)$$

where

$$\mathbf{Y}_n^* = \mathbf{Y}_{n+T}^* = \begin{pmatrix} \mathbf{Z}_n^*(\bar{p}) \\ \bar{p} \\ \vdots \\ \bar{p} \end{pmatrix}.$$

Here the set of $[(d+r)\times(d+r)]$-dimensional matrices $\tilde{\mathbf{A}}_n$ and the set of $(d+r)$-dimensional column vectors $\tilde{\mathbf{B}}_n$ are defined in terms of the partial derivatives given in Eq. (3):

$$\tilde{\mathbf{A}}_n = \begin{pmatrix} \mathbf{A}_n & \mathbf{B}_n^2 & \mathbf{B}_n^3 & \cdots & \mathbf{B}_n^r & \mathbf{B}_n^{r+1} \\ \mathbf{0} & 0 & 0 & \cdots & 0 & 0 \\ \mathbf{0} & 1 & 0 & \cdots & 0 & 0 \\ \mathbf{0} & 0 & 1 & \cdots & 0 & 0 \\ \vdots & \vdots & \vdots & \vdots & \vdots & \vdots \\ \mathbf{0} & 0 & 0 & \cdots & 1 & 0 \end{pmatrix}, \quad (7)$$

$$\tilde{\mathbf{B}}_n = \begin{pmatrix} \mathbf{B}_n^1 \\ 1 \\ 0 \\ \vdots \\ 0 \end{pmatrix}, \quad (8)$$

where $\mathbf{0}$ is the d-dimensional row vector of zeros. Because of the periodicity of the partial derivatives Eq. (3),

the $[(d+r)\times(d+r)]$-dimensional matrices $\tilde{\mathbf{A}}_n$ and the $(d+r)$-dimensional column vectors $\tilde{\mathbf{B}}_n$ are also periodic with a period T. One should note that this new state-plus-parameters dynamical equation reduces to the original linearized dynamics Eq. (4) if we consider only the first d components of Eq. (6). In particular, say that the periodic orbit $\mathbf{Z}_n^*$ is a saddle point with u unstable directions, s stable directions, and $d=u+s$. Then, in this state-plus-parameters representation, the u-dimensional linearized unstable subspace $E_u(\mathbf{Y}_n^*)$ in $\mathbb{R}^{(d+r)}$ is equivalent to the u-dimensional linearized unstable subspace $E_u(\mathbf{Z}_n^*)$ in $\mathbb{R}^d$, while the $(s+r)$-dimensional linearized stable subspace $E_s(\mathbf{Y}_n^*)$ in $\mathbb{R}^{(d+r)}$ is the direct sum of the equivalent s-dimensional linearized stable subspace $E_s(\mathbf{Z}_n^*)$ in $\mathbb{R}^d$ and the r-dimensional null space of $\tilde{\mathbf{A}}_{n-1}\tilde{\mathbf{A}}_{n-2}\cdots\tilde{\mathbf{A}}_{n-T}$ in $\mathbb{R}^{(d+r)}$.

The basic idea of our control algorithm is as follows. Given a periodic orbit $\mathbf{Y}_n^*=\mathbf{Y}_{n+T}^*$ with period T and u unstable directions, we either wait for the system trajectory to come close to the control region (which we will define later) of the desired periodic orbit $\mathbf{Y}_n^*$ or we can use the various targeting techniques [11–14] to bring the system trajectory near the control region of $\mathbf{Y}_n^*$. When the system state is in the control region, we will try to use u small parametric perturbations $p_n, p_{n+1}, \ldots, p_{n+(u-1)}$ to control the u unstable directions of the combined state-plus-parameters dynamics. In other words, with the u parametric controls in u iterates, we attempt to bring the deviation $\delta\mathbf{Y}_{n+u}=\mathbf{Y}_{n+u}-\mathbf{Y}_{n+u}^*$ to lie on the linearized stable subspace $E_s(\mathbf{Y}_{n+u}^*)$ of $\tilde{\mathbf{A}}_{n+u-1}\tilde{\mathbf{A}}_{n+u-2}\cdots\tilde{\mathbf{A}}_{n+u-T}$. After this is accomplished, the control can be set to $\bar{p}$ and the orbit will naturally approach the desired periodic orbit.

To get an explicit expression for the control parameters, let us consider u iterates of Eq. (6),

$$\begin{aligned}\mathbf{Y}_{n+u}-\mathbf{Y}_{n+u}^* &= \mathbf{\Phi}_{n,0}[\mathbf{Y}_n-\mathbf{Y}_n^*]+\mathbf{\Phi}_{n,1}\tilde{\mathbf{B}}_n(p_n-\bar{p})\\ &\quad+\mathbf{\Phi}_{n,2}\tilde{\mathbf{B}}_{n+1}(p_{n+1}-\bar{p})\\ &\quad+\cdots+\tilde{\mathbf{B}}_{n+(u-1)}(p_{n+(u-1)}-\bar{p}),\end{aligned}\tag{9}$$

where

$$\mathbf{\Phi}_{n,j}=\tilde{\mathbf{A}}_{n+u-1}\tilde{\mathbf{A}}_{n+u-2}\cdots\tilde{\mathbf{A}}_{n+j+1}\tilde{\mathbf{A}}_{n+j}\tag{10}$$

for $j=1,2,\ldots,(u-1)$, and $\mathbf{\Phi}_{n,u}\equiv\mathbf{I}$. We wish to place the deviation of the state vector $\delta\mathbf{Y}_{n+u}$ on the linearized stable subspace $E_s(\mathbf{Y}_{n+u}^*)$ at $\mathbf{Y}_{n+u}^*$. Assuming that this is accomplished, there exist $(s+r)$ coefficients $\alpha_1,\alpha_2,\ldots,\alpha_{s+r}$ such that

$$\begin{aligned}\mathbf{Y}_{n+u}-\mathbf{Y}_{n+u}^* &= \alpha_1\mathbf{v}_{n+u,1}+\alpha_2\mathbf{v}_{n+u,2}\\ &\quad+\cdots+\alpha_{s+r}\mathbf{v}_{n+u,s+r},\end{aligned}\tag{11}$$

where $\mathbf{v}_{n+u,1},\mathbf{v}_{n+u,2},\ldots,\mathbf{v}_{n+u,s+r}$ is any set of linearly independent unit vectors in $\mathbb{R}^{d+r}$ that spans $E_s(\mathbf{Y}_{n+u}^*)$. [Recall that $E_s(\mathbf{Y}_{n+u}^*)$ is the sum of the linearized stable subspace of $\mathbf{Z}_{n+u}^*$ and an r-dimensional null space.] Combining Eqs. (9) and (11), we then have $(d+r)$ equations with $(d+r)$ unknowns, $p_n,\ldots,p_{n+(u-1)},\alpha_1,\ldots,\alpha_{s+r}$. This can be solved to obtain an expression for the required control parameter

$$p_n=\bar{p}-\mathbf{K}_n^T[\mathbf{Y}_n-\mathbf{Y}_n^*],\tag{12}$$

where

$$\mathbf{K}_n^T=\kappa\mathbf{C}_n^{-1}\mathbf{\Phi}_{n,0}\tag{13}$$

and κ denotes an $(d+r)$-dimensional row vector whose first entry is one and whose remaining entries are all zeros. The $[(d+r)\times(d+r)]$ -dimensional matrix

$$\mathbf{C}_n=(\mathbf{\Phi}_{n,1}\tilde{\mathbf{B}}_n\vdots\mathbf{\Phi}_{n,2}\tilde{\mathbf{B}}_{n+1}\vdots\cdots\vdots\mathbf{\Phi}_{n,u-1}\tilde{\mathbf{B}}_{n+u-2}\vdots\tilde{\mathbf{B}}_{n+u-1}\vdots\mathbf{v}_{n+u,1}\vdots\mathbf{v}_{n+u,2}\vdots\cdots\vdots\mathbf{v}_{n+u,s+r})\tag{14}$$

is the "controllability" matrix with a similar meaning as in linear control theory such that the invertiblity of $\mathbf{C}_n$ implies the controllability of the periodic point $\mathbf{Y}_n^*$.

The construction of our control law Eq. (12) is based on the linearized Eq. (6) and in general we expect it to apply in the local neighborhood $N(\mathbf{Y}_n^*)$ near $\mathbf{Y}_n^*$. On the other hand, since we envision applying only small parametric perturbations $|p_n-\bar{p}|<\delta p_{max}$ in our control algorithm, we shall define the control region to be the set of all points $\mathbf{Y}_n$ within the slab,

$$\left|\mathbf{K}^T[\mathbf{Y}_n-\mathbf{Y}_n^*]\right|<\delta p_{max}.\tag{15}$$

For a given value of δp_{max}, the slab defined above intersects the local neighborhood $N(\mathbf{Y}_n^*)$ and its preimages. Points in the local neighborhood $N(\mathbf{Y}_n^*)$ will in general be controlled by Eq. (12) and we expect that, under forward applications of the control law Eq. (12), points in the preimages of $N(\mathbf{Y}_n^*)$ will eventually fall into the local neighborhood $N(\mathbf{Y}_n^*)$ and be controlled also. In our following numerical experiments, we have chosen to activate control according to Eq. (12) only when the values of $\mathbf{Y}_n$ are within the slab defined by Eq. (15) and the control parameter is left at its nominal value $\bar{p}$ otherwise. However, because of nonlinearity not included in the linearized Eq. (6), the control might not be able to bring the orbit to the desired periodic point for all points in the slab. In this case, the orbit will leave the slab and continue to wander chaotically as if there was no control. Since the orbit on the uncontrolled chaotic attractor is ergodic, after a chaotic transient [4], the orbit will once again enter the slab and may also be sufficiently close to $N(\mathbf{Y}_n^*)$ so that control is achieved.

In our derivation of the control law Eq. (12), although we only gave an explicit expression for the required parametric perturbation p_n at time n, we can, in principle, solve for all the control parameter values to be applied in the next u iterates $p_n,p_{n+1},\ldots,p_{n+u-1}$ from Eqs. (9) and (11). In the presence of noise, however, this is not a good idea (assuming $u>1$) since it does not take advantage of the opportunity to correct for the noise on each iterate. Therefore, we believe that, in the presence of noise, it is best to perform the calculation of p_n via Eq. (12) on each iterate.

In the paper by Dressler and Nitsche (see Ref. [3]),

past parametric dependence ($r = 1$ in their work) in the dynamical equation using delay coordinates embedding introduces a possible instability in their proposed control laws. For certain instances, it is possible that the required perturbations δp_n will grow in time even when the system state is arbitrary close to the periodic orbit. This instability will eventually force the orbit to exit the control region. Their solution is to apply controls only at every other steps instead of at every step so that δp_n can be reset to zero every other step. This is equivalent to eliminating the term in the control law that depends on the previous parameter. By utilizing the stable subspace $E_s(\mathbf{Y}_n^*)$ of the combined state-plus-parameters system, the required perturbations in our control law are linearly related to the deviations of the system state $\mathbf{Y}_n$ from the periodic orbit $\mathbf{Y}_n^*$. Thus the instability related to the increase of δp_n as in Dressler and Nitsche's method will not occur here.

III. NUMERICAL RESULTS

As a demonstration of our control method, we will use the Ikeda map as our first example. The Ikeda map describes the dynamics of a nonlinear optical cavity and is given by the following two-dimensional map in state space:

$$\mathbf{X}_{n+1} = \begin{pmatrix} u_{n+1} \\ v_{n+1} \end{pmatrix} = \begin{pmatrix} a_n + 0.9(u_n \cos\ s_n - v_n \sin\ s_n) \\ 0.9(u_n \sin\ s_n + v_n \cos\ s_n) \end{pmatrix}, \tag{16}$$

where $s_n = 0.4 - 6.0/(1 + u_n^2 + v_n^2)$. The magnitude and angle of the complex quantity $u_n + iv_n$ defines the amplitude and phase of the nth light pulse inside the cavity and a_n is the amplitude of the light pulse entering the cavity at time n. We will be using a_n as our control parameter in this numerical example. (For a detailed physical description of this map, refer to Hammel *et al.* [15].) At the nominal value of $a_n = \bar{a} = 1$, this dynamical system possesses a chaotic attractor with a Lyapunov dimension of 1.71. Embedded in this attractor, we have chosen the following three unstable periodic orbits for our numerical experiment [16]:

$$\mathbf{X}_{p2}^* = (u_{p2}^*, v_{p2}^*) = (0.509\ 84, -0.608\ 37)(0.621\ 60, 0.605\ 93),$$
$$\mathbf{X}_{p3}^* = (u_{p3}^*, v_{p3}^*) = (0.085\ 797, -0.883\ 23)(0.777\ 97, 0.767\ 17)(1.0140, -0.983\ 24),$$
$$\mathbf{X}_{p5}^* = (u_{p5}^*, v_{p5}^*) = (1.0447, 0.8002)(1.4917, -1.0775)(0.962\ 44, -1.6557)(0.394\ 62, -1.6138)(-0.221\ 33, -0.862\ 58).$$

As indicated by their subscripts, $\mathbf{X}_{p2}^*, \mathbf{X}_{p3}^*$, and $\mathbf{X}_{p5}^*$, are periodic points of Eq. (16) with period 2, 3, and 5, respectively.

To generate our time series $\{\xi_n\}$, we have chosen

$$\xi_n = u_n \tag{17}$$

as our experimental output [17]. In this case, the dynamical equation in delay coordinates Eq. (2) depends on a_n as well as on a_{n-1} ($r = 1$ in this case). Since we know the exact map Eq. (16) and the scalar output function Eq. (17), we can directly calculate the matrices $\mathbf{A}_n, \mathbf{B}_n^1$, and $\mathbf{B}_n^2$, appearing in Eq. (4). (As we have mentioned earlier, we can also obtain these matrices from time series using methods described in Refs. [5–10]. There is a good description in Ref. [3] to calculate the matrices $\mathbf{B}_n^1$ and $\mathbf{B}_n^2$ explicitly from experimental time series.) Choosing the maximal allowed perturbation δa_{max} to be 0.01, Figs. 1 and 2 summarize our main results for the Ikeda map.

We plot the values of the scale output ξ_n as a function of time n in Fig. 1(a) and we plot the applied parametric perturbations δp_n as a function of time n in Fig. 1(b). In these figures we turned on the control for the first periodic orbit $\mathbf{X}_{p2}^*$ at $n = 0$. After a chaotic transient (lasting until $n \simeq 3700$), the orbit $\mathbf{X}_{p2}^*$ was stablized. Then, we successive switched our control to the other two periodic orbits $\mathbf{X}_{p3}^*$ and $\mathbf{X}_{p5}^*$. The times at which the control was switched so as to stablize $\mathbf{X}_{p3}^*$ and $\mathbf{X}_{p5}^*$ are indicated in the Fig. 1 by arrows. In this figure, one can clearly see the flexibility offered by this method in controlling different periodic orbits embedded in a chaotic attractor reconstructed from time delay coordinates. Although the time to achieve control varied from case to case, in all cases,

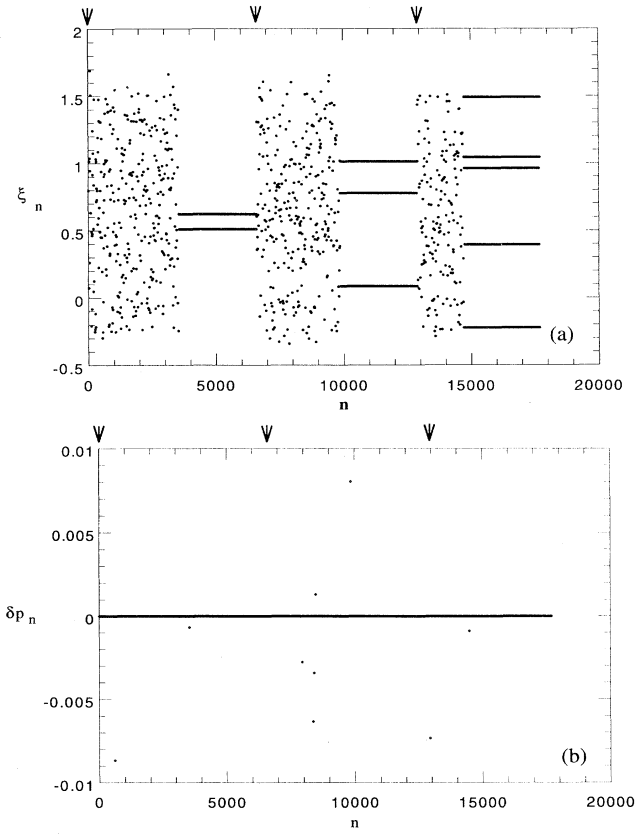

FIG. 1. Ikeda map: successive control of periodic points $\mathbf{X}_{p2}^*, \mathbf{X}_{p3}^*$, and $\mathbf{X}_{p5}^*$. (a) ξ vs n. (b) δp vs n. The arrows indicate the times of switching ($\bar{a} = 1$ and $\delta a_{max} = 0.01$).

the parametric control was able to bring the orbit close to the desired periodic point within a couple thousands of iterations.

This brings us to the issue of chaotic transient between the time when control is activated and the time when control is achieved. To study the time to achieve control, we begin with a large number $M_0 = 20\ 000$ of random initial orbits uniformly chosen on the attractor and we calculate the number of orbits remaining uncontrolled $M(n)$ as a function of time n. An orbit is considered to be under control when the required parametric perturbations δa_n remains within the range $[0, \delta a_{max}]$ for at least ten consecutive iterations. We expect the quantity $M(n)$ to decrease according to an exponential law

$$M(n) = M_0 e^{n/\langle n \rangle}, \tag{18}$$

where $\langle n \rangle$ is the average time to achieve control [4].

In Fig. 2(a) the periodic orbit being controlled is $\mathbf{X}^*_{p5}$ and we have plotted $\ln[M(n)/M_0]$ (denoted by a plus sign) as a function of n. From this graph, one can clearly see the expected exponential behavior for the time to achieve control. The slope of this graph gives the expected average time to achieved control $\langle n \rangle$ for a randomly chosen orbit on the attractor to be approximately 2500 iterations. To illustrate the effect of noise on this average time to achieve control, we plot three additional graphs Figs. 2(b)–2(d) showing again $\ln[M(n)/M_0]$ vs n for the cases where the output function Eq. (17) has an additional noise term

$$\xi_n = u_n + \epsilon \delta_n, \tag{19}$$

where δ_n is a random variable distributed uniformly between 0 and 1 and ϵ is the magnitude of the noise. Figure 2(b) shows data with $\epsilon = 10^{-5}$, Fig. 2(c) shows data with $\epsilon = 10^{-4}$, and Fig. 2(d) shows data with $\epsilon = 10^{-3}$. In these graphs, we can see that except for the case when $\epsilon = 10^{-3}$ the other three data sets, within expected errors, give the same average time to achieve control. The much slower convergence and the nonexponential behavior exhibited in the case with $\epsilon = 10^{-3}$ indicate that the noise is large enough so that many probably controllable orbits are being kicked away from the control region by noise.

To appreciate the importance of past parametric consideration in controlling systems using delay time coordinates, we now blindly assume that the surface of section map Eq. (2) depends only on the current parametric perturbation. Then, the required control parametric perturbation δa_n, for the Ikeda map in delay time coordinates with the output function given by $\xi_n = u_n$, would be

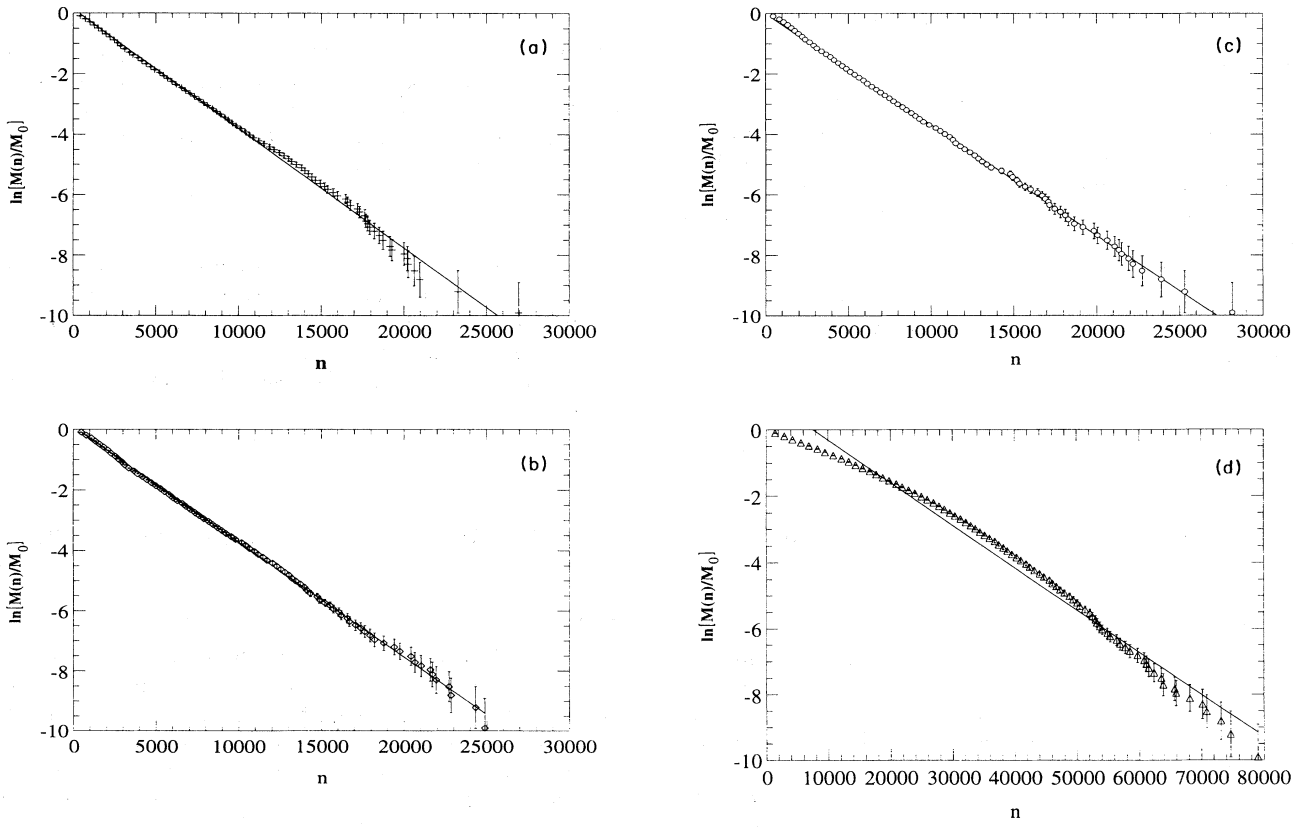

FIG. 2. Ikeda map: the natural logarithm of the fraction of uncontrolled orbits verse time. A sample of 20 000 initial orbits were chosen randomly over the attractor. An orbit is said to be controlled if $0 < \delta a_n < \delta a_{max}$ for at least ten consecutive iterations. The periodic point controlled is $\mathbf{X}^*_{p5}$. (a) + denotes data calculated with $\epsilon = 0$, (b) $\diamond$ denotes data calculated with $\epsilon = 10^{-5}$, (c) $\circ$ denotes data calculated with $\epsilon = 10^{-4}$ (d), and $\triangle$ denotes data calculated with $\epsilon = 10^{-3}$.

$$a_n - \bar{a} = -(1\ 0)[\mathbf{B}_n^1 \vdots \mathbf{v}_n^s]^{-1}\mathbf{A}_n[\mathbf{Z}_n - \mathbf{Z}_n^*], \quad (20)$$

where the two-dimensional column vector $\mathbf{B}_n^1$ and the two-dimensional matrix $\mathbf{A}_n$ are defined as in Eq. (3), $\mathbf{v}_n^s$ is the stable eigenvector of $\mathbf{A}_n\mathbf{A}_{n-1}\cdots\mathbf{A}_{n-(T-1)}$, and the delay vector $\mathbf{Z}_n$ is equal to $(\xi_n, \xi_{n-1}) = (u_n, u_{n-1})$. Figure 3 shows a section of the history of ξ_n for the two control methods: (a) Eq. (12) and (b) Eq. (20). In both cases, all parameters in the dynamical system were the same and we started the procedures with the same initial condition. The initial condition was chosen such that the initial orbit was within a distance of 10^{-4} away from the desired periodic orbit $\mathbf{X}_{p5}^*$. While our control method was able to further decrease the measured deviation $\xi_n - \xi_n^*$ down to the machine accuracy ($\approx 10^{-15}$), the control method without past parametric consideration was not able to stabilize the orbit. This result tells us that in typical cases when delay time coordinates are involved, parametric control methods must take past parametric dependences into consideration.

To demonstrate our method in a high-dimensional system, we will apply it to a periodically kicked mechanical system known as the kicked double rotor [4]. On the "stroboscopic surface of section," this mechanical system can be represented in state space by a four-dimensional map in the form

$$\mathbf{X}_{n+1} = \begin{pmatrix} \mathbf{\Theta}_{n+1} \\ \dot{\mathbf{\Theta}}_{n+1} \end{pmatrix} = \begin{pmatrix} \mathbf{W}_1\dot{\mathbf{\Theta}}_n + \mathbf{\Theta}_n \\ \mathbf{W}_2\dot{\mathbf{\Theta}}_n + f_n\mathbf{H}(\mathbf{\Theta}_{n+1}) \end{pmatrix}, \quad (21)$$

where $\mathbf{\Theta} = (\theta^1, \theta^2)^T$ are the two angular position coordinates, $\dot{\mathbf{\Theta}} = (\dot{\theta}^1, \dot{\theta}^2)^T$ are the corresponding angular velocities, and $\mathbf{H}(\mathbf{\Theta})$ is a nonlinear function. $\mathbf{W}_1$ and $\mathbf{W}_2$ are two constant matrices defined by the friction coefficients and moments of inertia of the rotor. We take as the control parameter of this system the strength of the kick f_n. Setting the nominal value of f_n to $\bar{f} = 9$ and the other parameters of the system to the ones in Ref. [4], the system processes a chaotic attractor with a Laypunov dimension of 2.838. To generate a scalar time series $\{\xi_n\}$, we will use

$$\xi_n = \theta_n^1. \quad (22)$$

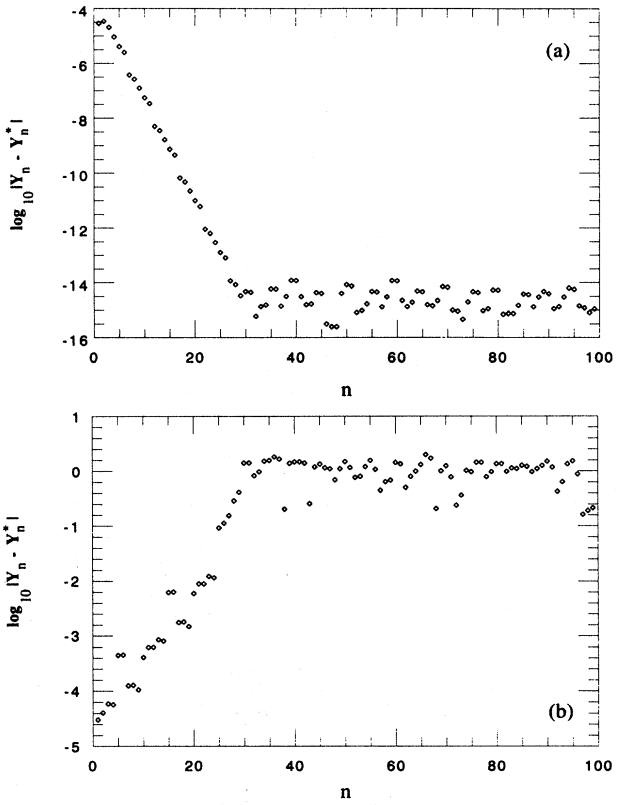

FIG. 3. Ikeda map: $\log_{10}|\mathbf{Y}_n - \mathbf{Y}_n^*|$ vs n. The periodic orbit being controlled is $\mathbf{X}_{p5}^*$. The test orbit was initialized within a radius of 10^{-4} away from the periodic point. (a) Control method introduced in this paper. (b) Control method without past parametric consideration.

With the choice of this output function, the corresponding dynamical equation in delay time coordinates Eq. (2) will depend on δf_n as well as on the three past parametric perturbations $\delta f_{n-1}, \delta f_{n-2}$, and δf_{n-3}, where $\delta f_n = f_n - \bar{f}$ ($r = 3$ in this case). The unstable periodic orbit

$$\mathbf{X}_R^* = (\theta_1^*, \theta_2^*, \dot{\theta}_1^*, \dot{\theta}_2^*)$$
$$= (3.1402, 0.481\ 05, -2.0364, 0.742\ 49)(2.3090, 0.565\ 80, 4.4182, 4.6514)(-0.834\ 74, -1.5220, -2.3818, -5.3938), \quad (23)$$

which we are attempting to control, is a period three orbit embedded in the attractor and it has two unstable directions and two stable directions. In our control algorithm, we have set the maximum allowed parameter perturbation δf_{max} to be equal to 1×10^{-4}. Figure 4 shows a history of the observed scalar output from the map as a function of time n. At time $n = 0$, the orbit first enters a neighborhood of radius 10^{-4} around the periodic point $\mathbf{X}_R^*$ and parametric control is activated at this time. One can see that the orbit quickly converges to the desired periodic orbit as n increases. As indicated by the small size of the neighborhood within which the orbit converges, we expected the average time to achieve control in this case to be quite large (on the order of 10^{12} iterations). This decrease in the size of the controllable region is mainly the consequence of using delay time embedding. In general, to uniquely determine a state of the system, we need to wait at least d iterations (d is the dimension of the system) to form the delay vector. Thus, even if the orbit is at a distance δ away from the periodic orbit at time n, the orbit will be at a distance of $\Lambda^d\delta$ away from the periodic orbit when the orbit can

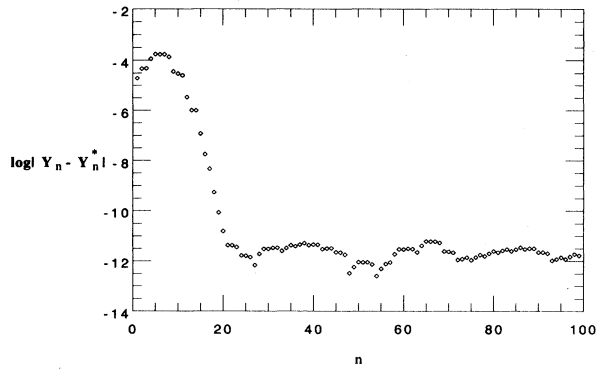

FIG. 4. Rotor map: $\log_{10}|\mathbf{Y}_n - \mathbf{Y}_n^*|$ vs n. The periodic orbit being controlled is $\mathbf{X}_R^*$. Parametric control is activated at $n = 0$. ($\bar{f} = 9$ and $\delta f_{max} = 0.1$)

be represented uniquely by the delay vector. (Here Λ is the largest multiplier of the periodic point.) Thus, typically, we should expect the size of the controllable region in delay time coordinates to be a factor of $(1/\Lambda)^d$ times smaller than the controllable region in regular state space coordinates. This effect will become more evident in higher-dimensional systems. With this long chaotic transient time, we believe that some kind of targeting techniques [11–14] will be essential in controlling these high-dimensional systems in delay time coordinates.

IV. CONCLUSION

In this paper, we have presented a method for control of chaotic systems using time delay coordinates. To take the dynamical dependence of past parameters into consideration, our parametric control law is constructed based on the combined dynamics of the state-plus-parameters system. In our numerical example using delay time coordinates, we have found that parametric control of unstable periodic points can only be achieved if we take past parametric perturbations into consideration (except the case when past parametric dependences are absent from the dynamical equation [23]). We found that our method is efficient in controlling and flexible in switching among different unstable periodic points embedded in an attractor of low dimension (the Ikeda map). However, while the method is able to control unstable periodic point embedded in a higher-dimensional attractor (the double rotor map), the chaotic transient time required for the orbit to come near the control region will in general be unacceptably long. While progress is being made in controlling high-dimensional systems [18], we believe that targeting and multivariant control [19] (using more than one control parameter) are two key issues in developing control schemes for high-dimensional systems with delay time coordinates.

APPENDIX

An alternative route to stabilizing unstable periodic orbits is via empirical proportional feedback (see Refs. [20,21]). In this method, one attempts to achive stabilization by an *ad hoc* feedback perturbation that is proportional to the difference between the state of the system and its desired periodic state (the parameter of the system is assumed to be fixed at its nominal value), i.e.,

$$\mathbf{Z}_{n+1} = \mathbf{G}(\mathbf{Z}_n, \bar{p}) - \mathbf{K}(\mathbf{Z}_n - \mathbf{Z}_n^*), \tag{A1}$$

where $\mathbf{K}$ is an adjustable gain matrix and $\mathbf{Z}_n^* = \mathbf{Z}_{n+T}^*$ is the desired periodic orbit. The stability of the periodic point $\mathbf{Z}_n^*$ depends on the spectrum of eigenvalues of the following stability matrix [22]:

$$\mathbf{L}(\mathbf{K}) = [\mathbf{A}_{n-1} - \mathbf{K}][\mathbf{A}_{n-2} - \mathbf{K}] \cdots [\mathbf{A}_{n-T} - \mathbf{K}], \tag{A2}$$

where $\mathbf{A}_n$ is the Jacobian of $\mathbf{G}(\mathbf{Z})$ [see Eq. (3)] evaluated at $\mathbf{Z}_n^*$ with p fixed at $\bar{p}$. The periodic orbit can be stabilized if the magnitude of the largest eigenvalue $\lambda_{max}(\mathbf{K})$ of $\mathbf{L}(\mathbf{K})$ is less than one. In most experimental cases, $\mathbf{K}$ is simply a scalar factor K multiplied by a projection operator $\mathbf{P}$. To illustrate this proportional feedback control scheme, we will agian use the Ikeda map Eq. (16) and the output scalar function $\xi_n = u_n$ to generate our time delay vector $\mathbf{Z}_n$. In Figs. 5(a) and 5(b), the projection operators that we have chosen for $\mathbf{K}$ are

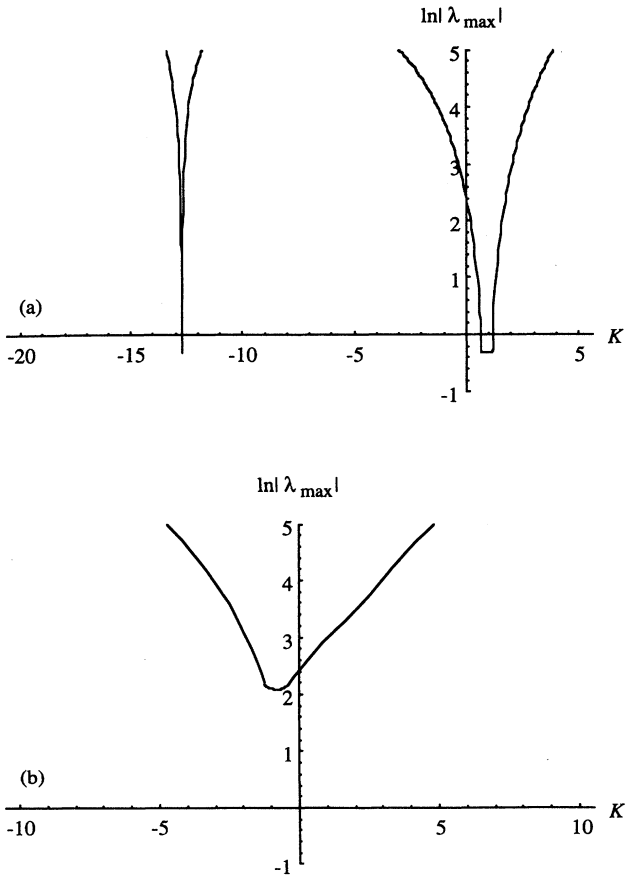

FIG. 5. Ikeda map: $\ln|\lambda_{max}(K)|$ vs K. (a) $\mathbf{K} = K\mathbf{P}_a$. (b) $\mathbf{K} = K\mathbf{P}_b$. The periodic orbit being considered is $\mathbf{X}_{p3}^*$ and it can be stabilized by the proportional feedback scheme for the values of K such that $\ln|\lambda_{max}(K)| \leq 0$.

(a) $\mathbf{P}_a = \begin{pmatrix} 1 & 0 \\ 0 & 0 \end{pmatrix}$ (b) $\mathbf{P}_b = \begin{pmatrix} 0 & 0 \\ 0 & 1 \end{pmatrix}$ and the periodic orbit being considered is $\mathbf{X}^*_{p3}$. In this graph, the logarithm of $|\lambda_{max}(K)|$ is plotted as a function of the scalar factor K. The periodic orbit $\mathbf{X}^*_{p3}$ can be stabilized by the proportional feedback scheme depending on the values of K. In particular, the proportional feedback scheme works for the values of K such that $|\lambda_{max}(K)| < 1$. In our first example, Fig. 5(a), there exist two small ranges of values of K such that the condition $|\lambda_{max}(K)| < 1$ [or, equivalently, $\ln|\lambda_{max}(K)| \leq 0$] is satisfied, while in our second example, Fig. 5(b), the condition is never satisfied in the range of values of K considered.

[1] E. Ott, C. Grebogi, and J. A. Yorke, Phys. Rev. Lett. **64**, 1196 (1990).

[2] F. Takens, in *Dynamical Systems and Turbulence*, edited by D. Rand and L. S. Young (Springer-Verlag, Berlin, 1981), p. 230.

[3] U. Dressler and G. Nitsche, Phys. Rev. Lett. **68**, 1 (1992).

[4] F. J. Romeiras, C. Grebogi, E. Ott, and W. P. Dayawansa, Physica D **58**, 165 (1992).

[5] J.-P. Eckmann and D. Ruelle, Rev. Mod. Phys. **57**, 617 (1985).

[6] E. J. Kostelich and J. A. Yorke, Phys. Rev. A **38**, 1649 (1988).

[7] E. J. Kostelich and J. A. Yorke, Physica D **41**, 183 (1990).

[8] D. P. Lathrop and E. J. Kostelich, Phys. Rev. A **40**, 4028 (1989).

[9] E. Kostelich, Physica D **58**, 138 (1992).

[10] D. Auerbach, P. Cvitanovič, J.-P. Eckmann, and G. Gunaratne, Phys. Rev. Lett. **58**, 2387 (1987).

[11] T. Shinbrot, E. Ott, C. Grebogi, and J. A. Yorke, Phys. Rev. Lett. **65**, 3215-3218 (1990); Phys. Rev. A **45**, 4165 (1992); Phys. Rev. Lett. **68**, 2863 (1992); Phys. Lett. A **169**, 349 (1992).

[12] E. Kostelich, C. Grebogi, E. Ott, and J. A. Yorke, Phys. Rev. E **47**, 305 (1993).

[13] E. Bradley, in *Lecture Notes Control and Information Sciences*, edited by G. Jacob and F. Lamnabhi-Lagarrigue (Springer, Berlin, 1991) No. 165, pp. 307–325.

[14] E. Barreto, E. Kostelich, E. Ott, C. Grebogi, and J. A. Yorke (unpublished).

[15] S. Hammel, C. K. Jones, and J. Maloney, J. Opt. Soc. Am. B, **2**, 552 (1985).

[16] The periodic points are found numerically using the program written by H. E. Nusse, J. A. Yorke, and E. Kostelich, DYNAMICS: NUMERICAL EXPLORATIONS, 1992.

[17] Other linear combinations of u_n and v_n, e.g., $\xi_n = u_n + v_n$, were also considered. Results were similar as long as the controllability matrix C_n is not too close to being singular.

[18] D. Auerbach, C. Grebogi, E. Ott, and J. A. Yorke, Phys. Rev. Lett. **69**, 3479 (1992).

[19] E. Barreto *et al.* (unpublished).

[20] K. Pyragas, Phys. Lett. A **170**, 421 (1992).

[21] K. Pyragas, Phys. Lett. A **181**, 203 (1993).

[22] Since the periodic orbit $\mathbf{Z}^*_n$ is of period T, i.e., $\mathbf{A}_n = \mathbf{A}_{n+T}$, there will be a total of T different L_j's. However, since the determint of a product of matrices is the product of the determint of the same matrices, the spectrum of eigenvalues for all $\mathbf{L}_j$ with $1 \leq j \leq T$ is the same.

[23] These include the numerous successful implementations of the original OGY method in controlling various experimental time series (see Refs. [24–31]). In these examples, the relevant dynamics can in general be described by one-dimensional return maps, which are insensitive to past parametric variations.

[24] W. Ditto, S. N. Rauseo, and M. L. Spano, Phys. Rev. Lett. **65**, 3211 (1990).

[25] J. Singer, Y.-Z. Wang, and H. H. Bau, Phys. Rev. Lett. **66**, 1123 (1991).

[26] A. Garfinkel, M. Spano, W. Ditto, and J. Weiss, Science **257**, 1230 (1992).

[27] E. R. Hunt, Phys. Rev. Lett. **67**, 1953 (1991).

[28] Z. Gills, C. Iwata, R. Roy, I. Schwartz, and I. Triandaf, Phys. Rev. Lett. **69**, 3169 (1992).

[29] C. Reyl, L. Flepp, R. Badii, and E. Brun, Phys. Rev. E **47**, 267 (1993).

[30] V. Petrov, V. Gáspár, J. Masere, and K. Showalter, Nature **361**, 240 (1993).

[31] S. Schiff, K. Jerger, D. G. Duong, T. Chang, M. L. Spano, and W. Ditto, Nature **370**, 615 (1994).